

Article

Optimized Pore Structures of Hierarchical HY Zeolites for Highly Selective Production of Methyl Methoxyacetate

Fei Chen [†], Dongxi Zhang [†], Lei Shi ^{*†} , Yan Wang and Guangwen Xu ^{*}

Institute of Industrial Chemistry and Energy Technology, Shenyang University of Chemical Technology, Shenyang 110142, China; cf19950622@163.com (F.C.); zhang_dongxi19@163.com (D.Z.); wangyan_melody@126.com (Y.W.)

* Correspondence: shilei1982@dicp.ac.cn (L.S.); gw Xu@syuct.edu.cn (G.X.); Tel.: +86-024-89388216 (L.S.)

[†] These authors are equal to this work.

Received: 19 September 2019; Accepted: 14 October 2019; Published: 18 October 2019



Abstract: Several organic templates were introduced during acid or alkaline treatment to optimize pore structures of hierarchical HY zeolites. The influences of category and concentration of templates on the pore structures and acidity of hierarchical HY zeolites were systemically studied. The N₂ adsorption-desorption showed that the micropore amount of the optimized HY zeolites obviously increased, while both the large mesopore size and amount remained almost unchanged. The XRD and NH₃-TPD revealed that the optimized HY zeolites exhibited higher relative crystallinity and medium-strong acid sites amount than those of hierarchical HY zeolites produced without the addition of templates. The optimized HY zeolites were used for the synthesis of methyl methoxyacetate (MMAc) from dimethoxymethane (DMM) carbonylation. In comparison with parent HY, the conversion and the selectivity clearly increased from 36.43% to 96.32% and from 11.06% to 92.35%, respectively. The stability of the optimized zeolite was also conducted under the same conditions. The conversion and the selectivity remained nearly unchanged even through 24 h reaction, showing that the performance was extremely stable. The TG-DTA and GC-MS also indicated that the generation of coke was effectively inhibited. This catalyst treatment method, which is facile and highly efficient, provided a route for producing mesoporous zeolites.

Keywords: Hierarchical zeolites; Pore directing agents (PDAs); Dimethoxymethane (DMM); carbonylation; Methyl methoxyacetate (MMAc)

1. Introduction

Hierarchical zeolites, which have microporous and mesoporous structure, have received wide attention in the past decade, since they display superior catalytic activity compared to traditional microporous zeolites in several reactions [1–3]. For instance, the performance and catalyst lifetime for catalytic cracking of large molecules are significantly improved with hierarchical zeolites in place of micropore catalysts due to increased diffusion [4]. Hierarchical ZSM-5 zeolite employed in the benzylation of benzyl alcohol with benzene reaction can clearly enhance the mass transfer and improve the product selectivity [5]. Furthermore, the activity of hierarchical SAPO-34 for the MTO process is obviously enhanced [6].

Methyl methoxyacetate (MMAc) is one of the significant fine chemicals and can be applied to produce protectants, pharmaceuticals, and vitamin B6 [7,8]. MMAc is also an important intermediate for the preparation of ethylene glycol [9], a bulk chemical widely employed in polyester fiber, antifreeze, surface active agents, and textiles [10].

In our previous study [11], a sequential acid and alkaline solution treatment was applied for the preparation of hierarchical HY zeolites with greater mesopore volume and surface area. The pretreated samples displayed much higher catalytic activity and stability than those of parent HY zeolites for the dimethoxymethane (DMM) carbonylation to MMAc because of higher mass transfer efficiency and less carbon deposition, and the conversion of DMM was closely relevant to the amount of medium-strong acid sites. However, the selective extraction of aluminum and silicon from the framework caused the formation of vacancies and amorphous species [12], leading to a decrease of the relative crystallinity. Besides, the alkaline treatment could influence the state of framework aluminum [13], resulting in the decrease of the acidity. Therefore, it was important to protect crystallinity and acidity during acid or alkaline treatment.

The introduction of organic templates was an effective method to protect crystallinity and acidity during acid or alkaline treatment [14–22]. These templates, which are named as external pore directing agents (PDAs) [15], could be absorbed on the external surface of zeolites. Tetrapropyl ammonium (TPA^+) or tetramethyl ammonium (TMA^+) have been proved to be helpful in the formation of directing mesopores during the desilication process [19]. Another branch of excellent PDAs involved cationic surfactants such as cetyltrimethylammonium (CTA^+) [18,19]. This surfactant could promote a reassembly of the dissolved aluminum and silicon species [19]. In 1995, Ankica Čížmek et al. [14] first investigated the desilication of high-silica ZSM-5 zeolites in the presence of TPA^+ . The results indicated that the introduction of TPA^+ could control the dissolution of ZSM-5 and thus protect the framework silica. Petra E. de Jongh et al. [20] reported that templated ZSM-5, ZSM-12, and Beta zeolites could introduce mesopores via sodium hydroxide treatment, without changing crystallinity and acidity. Javier Pérez-Ramírez et al. [15,16] revealed that the addition of TPA^+ during alkaline treatment could obtain mesoporous Beta and USY zeolites with high crystallinity. Their studies also indicated that the tetraalkylammonium cations with long alkyl chains were more conducive to the formation of zeolite pores [15,17]. Javier Garcia-Martinez et al. [22] demonstrated that the introduction of surfactants during acid treatment could lead to the generation of the ordered mesoporous zeolites. Furthermore, many articles and reviews have reported some synthetic strategies and characterization methods of hierarchical materials. Monoj Ghosh et al. [23] prepared mesoporous TiO_2 nanofibers via a facile gas jet fiber spinning process. The porous structure was controlled by using a polymer template (polyvinylpyrrolidone) and sol-gel chemistry. Liu et al. [24] reviewed the synthesis strategies for hierarchical zeolites through the “direct synthesis” route, using a series of templates. Bai et al. [25] reviewed various synthesis methods in the production of hierarchical zeolites by means of mesopore, mesopore-free and demetallization strategies. K.S.W. Sing et al. [26] summarized characterization methods and physisorption data for the determination of porosity and surface area.

In this work, commercial HY zeolite ($\text{Si}/\text{Al} = 2.7$) was employed as the primary precursor. Several organic templates (tetrapropyl ammonium bromide (TPABr), tetrapropyl ammonium hydroxide (TPAOH), tetraethyl ammonium hydroxide (TEAOH), and tetramethyl ammonium hydroxide (TMAOH)) were introduced during acid or alkaline treatment to optimize pore structures of hierarchical HY zeolites. The effects of category and concentration of templates on the relative crystallinity, pore structures, and acidity of hierarchical HY zeolites were systemically investigated and discussed, combined with XRD, N_2 adsorption-desorption and NH_3 -TPD results. The carbonylation of DMM to MMAc was employed as a model reaction to assess the parent HY and the optimized HY zeolites, and the differences in the catalytic activity were related to physiochemical properties of the optimized HY zeolites. The catalytic stability of parent HY, HY produced without the addition of templates, as well as HY produced with 0.10 mol/L TPAOH were also carried out under the same conditions. The coke generation and coke species of the used HY zeolites after 24 h reaction was identified by TG-DTA and GC-MS analysis. This optimized HY zeolite with high activity, selectivity, and excellent stability exhibited enormous potential for industrial production of MMAc from DMM carbonylation.

2. Results and Discussion

2.1. XRD Analysis

The power XRD patterns of parent HY, HY-H₄EDTA (only treated by 0.11 mol/L H₄EDTA), HY-H₄EDTA-TPABr (by 0.11 mol/L H₄EDTA and 0.10 mol/L TPABr), HY-H₄EDTA-NH₄OH (further treated by 0.10 mol/L NH₄OH founded on HY-H₄EDTA), and HY-H₄EDTA-NaOH (by 0.10 mol/L NaOH) are shown in Figure 1A. The relative crystallinity of HY-H₄EDTA, HY-H₄EDTA-TPABr, HY-H₄EDTA-NH₄OH, and HY-H₄EDTA-NaOH, which were calculated by comparing the relative intensity divided by the reference at 2θ of 23.58°, were 58.39%, 61.80%, 53.50%, and 40.98%, respectively, supposing that the reference HY crystallinity was 100% (Table 1). As compared with the reference HY zeolite, the crystallinity of HY-H₄EDTA significantly decreased due to the formation of vacancies and amorphous aluminum species during the dealumination process [12]. After dealumination via H₄EDTA, further desilication through NH₄OH or NaOH solution caused more severe crumbling of zeolite crystals, owing to the breakage of Si-O-Si and Si-O-Al by OH⁻ [27,28]. In comparison with HY-H₄EDTA, the crystallinity of HY-H₄EDTA-TPABr slightly improved to 61.80%, indicating that the introduction of TPABr during H₄EDTA treatment could effectively protect the crystallinity of zeolites. The introduced TPA⁺ cations could be adsorbed on the external surface of zeolites through a monolayer adsorption mode [15,29]. On the one hand, the adsorbed TPA⁺ cations blocked most of the usable outer surface and thus controlled the dissolution of the zeolite crystals [15,19]. On the other hand, the adsorbed TPA⁺ cations also largely restrained the surface realumination, leading to the permanent departure of aluminum species from zeolite crystals [15]. Accordingly, HY-H₄EDTA-TPABr zeolite treated by H₄EDTA and TPA⁺ exhibited greater crystallinity than that of HY-H₄EDTA zeolite handled by pure H₄EDTA.

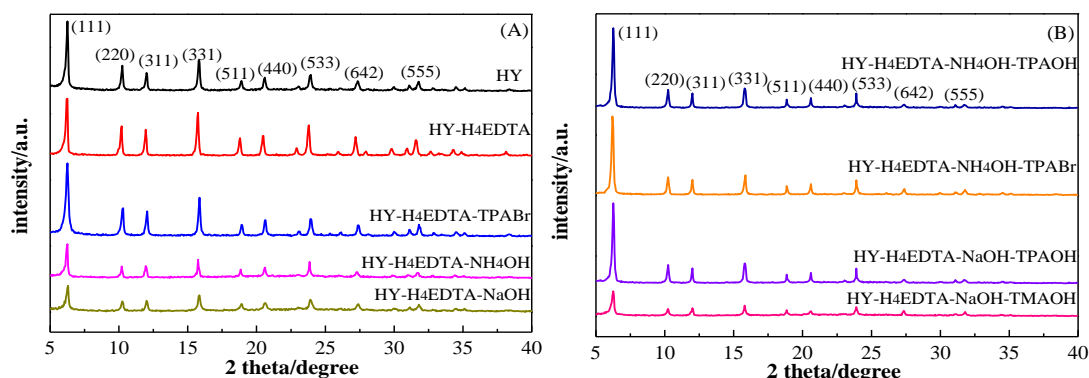


Figure 1. XRD patterns of the parent HY and the optimized hierarchical HY zeolites (A) and (B).

As displayed in Figure 1B and Table 1, the relative crystallinity of HY-H₄EDTA-NH₄OH-TPAOH (further treated by 0.10 mol/L NH₄OH and 0.10 mol/L TPAOH founded on HY-0.11), HY-H₄EDTA-NH₄OH-TPABr (by 0.10 mol/L NH₄OH and 0.10 mol/L TPABr), HY-H₄EDTA-NaOH-TPAOH (by 0.10 mol/L NaOH and 0.10 mol/L TPAOH), and HY-H₄EDTA-NaOH-TMAOH (by 0.10 mol/L NaOH and 0.10 mol/L TMAOH) were 79.82%, 79.39%, 60.08%, and 48.47%, respectively. When HY-0.11 was only handled by 0.10 mol/L NH₄OH for desilication, the crystallinity of HY-H₄EDTA-NH₄OH was only 53.50%. With the addition of 0.10 mol/L TPAOH or TPABr during NH₄OH treatment, the crystallinity of HY-H₄EDTA-NH₄OH-TPAOH and HY-H₄EDTA-NH₄OH-TPABr obviously increased to 79.82% and 79.39%, respectively. Similarly, with only 0.10 mol/L NaOH for desilication, the crystallinity of HY-H₄EDTA-NaOH was as low as 40.98%. When 0.10 mol/L TPAOH or TMAOH was added in NaOH solution, the crystallinity of HY-H₄EDTA-NaOH-TPAOH and HY-H₄EDTA-NaOH-TMAOH clearly increased to 60.08% and 48.47%, respectively. The above results demonstrate that the addition of TPA⁺ or TMA⁺ in either NH₄OH or NaOH treatment evidently protected the crystallinity of zeolites.

According to previous reports [15,29], the TPA⁺ or TMA⁺ molecules were absorbed by zeolites via a monolayer adsorption mode, sealing off a majority of the available outer surface and thereby protecting the zeolite structure [18]. Furthermore, the absorbed TPA⁺ or TMA⁺ species could largely suppress zeolite recrystallization during alkaline treatment, resulting in the generation of mono-phase, highly crystalline in the zeolite crystals [16]. Therefore, hierarchical HY zeolites optimized by TPA⁺ or TMA⁺ displayed higher crystallinity.

Table 1. The crystallinity and acidity distribution of pretreated zeolites.

Catalysts	Crystallinity/%	Weak Acid	Medium-Strong Acid	Total Acid
		Amount/mmol·g ⁻¹	Amount/mmol·g ⁻¹	
		T ₁ /370–550 K	T ₂ /550–850K	
HY	100	1.68	0.53	2.21
HY-H ₄ EDTA	58.39	0.72	0.21	0.93
HY-H ₄ EDTA-TPABr	61.80	0.59	0.32	0.91
HY-H ₄ EDTA-NH ₄ OH	53.50	0.63	0.20	0.83
HY-H ₄ EDTA-NH ₄ OH-0.05TPAOH	–	0.61	0.25	0.86
HY-H ₄ EDTA-NH ₄ OH-TPAOH	79.82	0.60	0.31	0.91
HY-H ₄ EDTA-NH ₄ OH-TPABr	79.39	–	–	–
HY-H ₄ EDTA-NH ₄ OH-0.20TPAOH	–	0.59	0.32	0.91
HY-H ₄ EDTA-0.20NH ₄ OH-TPAOH	–	0.62	0.26	0.88
HY-H ₄ EDTA-NaOH	40.98	0.69	0.07	0.76
HY-H ₄ EDTA-NaOH-TPAOH	60.08	0.63	0.23	0.86
HY-H ₄ EDTA-NaOH-TMAOH	48.47	–	–	–

As shown in Table 1, the categories of organic templates also influenced the crystallinity of zeolites during alkaline treatment. The HY-H₄EDTA-NH₄OH-TPAOH (79.82%) exhibited similar crystallinity to that of the HY-H₄EDTA-NH₄OH-TPABr (79.39%), showing that the anion of templates had almost no effect on the crystallinity. However, it was obvious that the crystallinity of HY-H₄EDTA-NaOH-TPAOH (60.08%) was much higher than that of HY-H₄EDTA-NaOH-TMAOH (48.47%), demonstrating that the cation with short alkyl chain (TMA⁺) was not beneficial to protecting crystallinity because a short alkyl chain could not generate a tightly packed adsorption layer [8], resulting in a weak protection role of the zeolitic structure. Hence, HY-H₄EDTA-NaOH-TPAOH zeolite treated by NaOH and TPA⁺ exhibited higher crystallinity than that of HY-H₄EDTA-NaOH-TMAOH zeolite handled by NaOH and TMA⁺.

2.2. NH₃-TPD Analysis

The acidity and acid amounts of optimized HY zeolites was gauged by NH₃-TPD analysis and shown in Figure 2A,B. All the zeolites exhibited two desorption peaks of NH₃. The low temperature desorption peak was ascribed to weak acid centers, while the high temperature peak was assigned to medium-strong acid centers [30–35]. The acid amount was computed in the light of the desorbed NH₃ amount and is listed in Table 1. The weak acid amounts of HY, HY-H₄EDTA, HY-H₄EDTA-TPABr, HY-H₄EDTA-NH₄OH, HY-H₄EDTA-NaOH, HY-H₄EDTA-NH₄OH-0.05TPAOH, HY-H₄EDTA-NH₄OH-TPAOH, HY-H₄EDTA-NH₄OH-0.20TPAOH, HY-H₄EDTA-0.20NH₄OH-TPAOH, and HY-H₄EDTA-NaOH-TPAOH were 1.68, 0.72, 0.59, 0.63, 0.69, 0.61, 0.60, 0.59, 0.62, and 0.63 mmol·g⁻¹, while their medium-strong acid amounts were 0.53, 0.21, 0.32, 0.20, 0.07, 0.25, 0.31, 0.32, 0.26, and 0.23 mmol·g⁻¹. As compared with the parent HY zeolite, the acid amount obviously reduced with H₄EDTA treatment. After dealumination and further desilication by NH₄OH or NaOH, the amount of acid also clearly dropped. In comparison with HY-H₄EDTA, the HY-H₄EDTA-TPABr zeolite treated by H₄EDTA and TPABr resulted in a decrease of the weak acid amount from 0.72 to 0.59 mmol·g⁻¹ and an increase of the medium-strong acid amount from 0.21 to 0.32 mmol·g⁻¹. When the HY-H₄EDTA zeolite was only treated by 0.10 mol/L NH₄OH, the weak and medium-strong acid amounts were 0.63 and 0.20 mmol·g⁻¹, respectively. With improving the concentration of TPAOH from 0 to 0.10 mol/L, the weak acid amount decreased and showed 0.60 mmol·g⁻¹, while the medium-strong acid amount increased and exhibited 0.32 mmol·g⁻¹ at 0.10 mol/L TPAOH. Further enhancing the TPAOH concentration to 0.20 mol/L, the amount of weak acid centers slightly dropped from 0.60 to 0.59 mmol·g⁻¹, yet the

amount of medium-strong acid sites briefly improved from 0.31 to 0.32 $\text{mmol}\cdot\text{g}^{-1}$. The change trend of the total acid amount was consistent with that of the medium-strong acid amount and constantly increased and exhibited the maximum value ($0.92 \text{ mmol}\cdot\text{g}^{-1}$) at 0.20 mol/L TPAOH. When the TPAOH concentration was fixed at 0.10 mol/L, the amount of weak acid centers slowly increased from 0.60 to 0.62 $\text{mmol}\cdot\text{g}^{-1}$, and the amount of medium-strong acid sites gradually decreased from 0.32 to 0.26 $\text{mmol}\cdot\text{g}^{-1}$, with improvements in the NH_4OH concentration from 0.10 to 0.20 mol/L. The above results clearly indicate that the introduction of TPAOH during the dealumination or desilication process could increase the medium-strong acid amount of as-treated HY zeolites. Furthermore, the acid amount was closely related to the concentration of TPAOH, and higher TPAOH concentration led to a greater medium-strong acid amount. It has been reported [36] that the medium-strong acid amount is associated with the amount of framework aluminum with tetrahedral coordination. As discussed above, the introduction of TPA^+ could control the dissolution of the zeolite crystal and protect the framework aluminum, leading to an increase of the medium-strong acid amount.

After dealumination by H_4EDTA , the peak of weak acid sites transformed from 468 to 443 K, demonstrating that the intensity of weak acid centers dropped. After further desilication by 0.10 mol/L NH_4OH or NaOH , the peak changed to 450 or 440 K. The desorption temperature of the medium-strong acid peak dropped from 670 to 618 K when the parent HY zeolite was only treated by H_4EDTA . After further desilication by 0.10 mol/L NH_4OH , the second peak shifted to 626 K. With desilication by the same concentration of NaOH , the medium-strong acid peak practically vanished. It was obvious that the intensity of acid sites decreased after dealumination or desilication. As compared with $\text{HY}\text{-H}_4\text{EDTA}$, the two desorption peaks of $\text{HY}\text{-H}_4\text{EDTA}\text{-TPABr}$ zeolite shifted to a higher temperature range, suggesting that the strength of both weak acid and medium-strong acid sites clearly increased. This result indicates that the introduction of TPAOH could protect acidity during acid treatment. In comparison with $\text{HY}\text{-H}_4\text{EDTA}\text{-NH}_4\text{OH}$ and $\text{HY}\text{-H}_4\text{EDTA}\text{-NaOH}$, the desorption temperature remained nearly unchanged (450 and 626 K, respectively) with the variation of TPAOH concentration, indicating that the addition of TPAOH could not change the strength of acid sites during alkaline treatment. The above results are in good agreement with the literature reports [20].

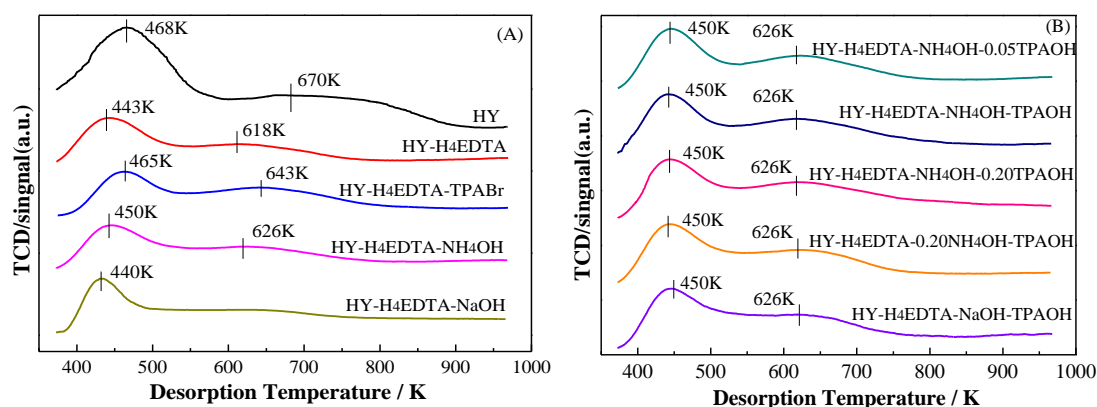


Figure 2. NH_3 -TPD analysis of the parent HY and the optimized hierarchical HY zeolites (A) and (B).

2.3. N_2 Adsorption-Desorption Analysis

The isotherms of HY, $\text{HY}\text{-H}_4\text{EDTA}$, $\text{HY}\text{-H}_4\text{EDTA}\text{-TPABr}$, $\text{HY}\text{-H}_4\text{EDTA}\text{-NH}_4\text{OH}$, and $\text{HY}\text{-H}_4\text{EDTA}\text{-NH}_4\text{OH}\text{-TPAOH}$ are exhibited in Figure 3. The pretreated samples displayed Type IV isotherm, including the hysteresis loop at P/P_0 greater than 0.4, which demonstrated the presence of mesoporous structure [21].

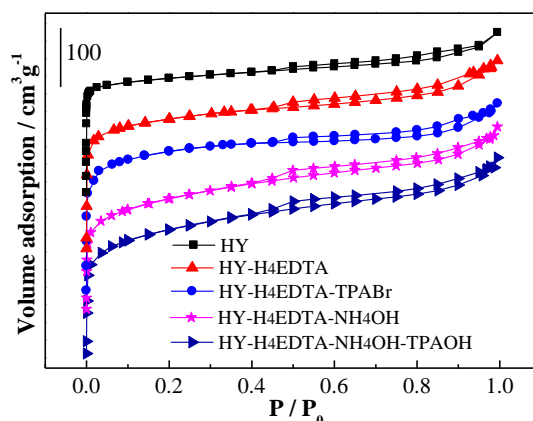


Figure 3. N_2 adsorption-desorption isotherms of the parent HY and the optimized hierarchical HY zeolites.

The micropore sizes distribution determined by the Horváth–Kawazoe (HK) method as well as the mesopore sizes distribution calculated by the Barrett–Joyner–Halenda (BJH) method [23–26] are displayed in Figure 4A,B. As exhibited in Figure 4A, all the zeolites exhibited a unimodal in the microporous area. The parent HY displayed a micropore size of 0.56 nm with $1.56 \text{ cm}^3 \text{ g}^{-1} \text{ nm}^{-1}$ intensity. When HY zeolite was treated by 0.11 mol/L H_4EDTA , the micropore size of HY- H_4EDTA dropped to 0.50 nm, while the intensity obviously enhanced to $2.53 \text{ cm}^3 \text{ g}^{-1} \text{ nm}^{-1}$, which was extremely greater than that of HY, indicating that the amount of micropore clearly improved. After dealumination and further desilication by 0.10 mol/L NH_4OH , the micropore size of HY- $H_4EDTA-NH_4OH$ slightly enhanced to 0.59 nm, and the peak intensity markedly dropped to $1.21 \text{ cm}^3 \text{ g}^{-1} \text{ nm}^{-1}$, showing that the micropore amount evidently decreased with the alkaline treatment. As compared with HY- H_4EDTA , the peak intensity of HY- $H_4EDTA-TPABr$ increased to $2.62 \text{ cm}^3 \text{ g}^{-1} \text{ nm}^{-1}$, although the micropore size slightly dropped to 0.47 nm, suggesting that the micropore amount increased with the introduction of TPA^+ during acid treatment. In comparison with HY- $H_4EDTA-NH_4OH$, the micropore size of HY- $H_4EDTA-NH_4OH-TPAOH$ remained nearly unchanged (0.58 nm), while the intensity rapidly increased to $1.52 \text{ cm}^3 \text{ g}^{-1} \text{ nm}^{-1}$, indicating that the addition of TPA^+ could also enhance the micropore amount during alkaline treatment. As shown in Figure 4B, the reference HY exhibited two peaks in mesopore area. The first peak was ascribed to small mesoporous (3.41 nm), while the second peak associated well with large mesoporous (17.51 nm) [11]. The intensity corresponding to these two peaks were 0.10 and $0.09 \text{ cm}^3 \text{ g}^{-1} \text{ nm}^{-1}$, respectively. When HY zeolite was treated by 0.11 mol/L H_4EDTA , the small mesopore size of HY- H_4EDTA remained almost the same, yet the intensity dropped to $0.09 \text{ cm}^3 \text{ g}^{-1} \text{ nm}^{-1}$; the large mesoporous rose to 18.32 nm with $0.10 \text{ cm}^3 \text{ g}^{-1} \text{ nm}^{-1}$ intensity. After dealumination and further desilication by 0.10 mol/L NH_4OH , the small mesoporous of HY- $H_4EDTA-NH_4OH$ disappeared, while the large mesopore size decreased to 17.44 nm with $0.11 \text{ cm}^3 \text{ g}^{-1} \text{ nm}^{-1}$ intensity. As compared with HY- H_4EDTA , the small mesoporous of HY- $H_4EDTA-TPABr$ vanished, while both the large mesopore size and intensity stayed at constant values (18.34 nm and $0.10 \text{ cm}^3 \text{ g}^{-1} \text{ nm}^{-1}$). Similarly, in comparison with HY- $H_4EDTA-NH_4OH$, the small mesoporous of HY- $H_4EDTA-NH_4OH-TPAOH$ also disappeared, while the large mesopore size and intensity also remained nearly unchanged (17.43 nm and $0.10 \text{ cm}^3 \text{ g}^{-1} \text{ nm}^{-1}$).

The above results indicate that 0.11 mol/L H_4EDTA treatment could increase the amount of micropore and large mesopore but reduce micropore sizes due to the formation of amorphous aluminum species [12]. Dealumination and further desilication by 0.10 mol/L NH_4OH led to the increase of micropore size but the decrease of large mesopore size as well as micropore amount. With the introduction of TPA^+ during H_4EDTA and NH_4OH treatment, the micropore amount clearly increased, while both the large mesopore size and amount remained almost unchanged, showing that

the added TPA^+ largely protected microporosity. This result is consistent with that of the literature reports [16] and is further proved by the following pore volumes analysis.

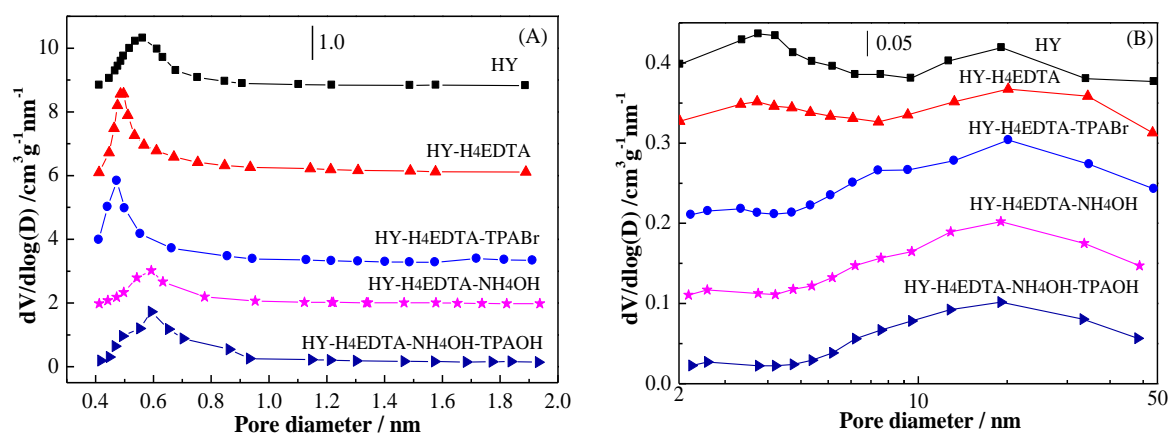


Figure 4. The micropore pore size (A) and mesopore pore size (B) distribution of the parent HY and the optimized hierarchical HY zeolites.

The characterization results of pore volumes and BET surface areas are exhibited in Table 2. The external surface area, computed by t-plot method [37] and associated with mesoporous surface area [38], of HY, HY- H_4EDTA , HY- $\text{H}_4\text{EDTA-TPABr}$, HY- $\text{H}_4\text{EDTA-NH}_4\text{OH}$, and HY- $\text{H}_4\text{EDTA-NH}_4\text{OH-TPAOH}$ were 126, 264, 138, 237, and 158 m^2/g , respectively. The corresponding mesopore volumes were 0.13, 0.24, 0.20, 0.26, and 0.22 cm^3/g , respectively. The micropore volumes of these samples were 0.27, 0.22, 0.26, 0.19, 0.23 cm^3/g , respectively. The above results demonstrate that the mesoporous surface area and volume of HY- H_4EDTA were approximately twofold larger than those of the parent HY zeolite, while the micropore volume slightly decreased, indicating that H_4EDTA treatment led to the collapse of microporous and caused the formation of mesoporous [38,39]. Dealumination and further desilication by 0.10 mol/L NH_4OH resulted in the decrease of mesoporous surface area and micropore volume but the increase of mesopore volume, showing that NH_4OH treatment further resulted in the generation of mesoporous [27]. In comparison with HY- H_4EDTA , the mesoporous surface area and volume of HY- $\text{H}_4\text{EDTA-TPABr}$ clearly decreased, while the micropore volume slightly increased. A similar result was also observed during alkaline treatment in the presence of TPA^+ . The HY- $\text{H}_4\text{EDTA-NH}_4\text{OH-TPAOH}$ exhibited smaller mesoporous surface area and volume as well as higher micropore volume than those of HY- $\text{H}_4\text{EDTA-NH}_4\text{OH}$. These results were in good agreement with the previous discussion, which indicates that the introduction of TPA^+ could effectively protect microporous structure during acid or alkaline treatment.

Table 2. Characterization results of pore volumes and BET surface areas of pretreated zeolites.

Catalysts	Surface Area (m^2/g)			Pore Volume (cm^3/g)		
	Total ^a	Micro ^b	External Area ^c	Total ^d	Micro ^e	Meso ^f
HY	682	556	126	0.40	0.27	0.13
HY- H_4EDTA	816	552	264	0.46	0.22	0.24
HY- $\text{H}_4\text{EDTA-TPABr}$	852	714	138	0.46	0.26	0.20
HY- $\text{H}_4\text{EDTA-NH}_4\text{OH}$	699	462	237	0.45	0.19	0.26
HY- $\text{H}_4\text{EDTA-NH}_4\text{OH-TPAOH}$	722	564	158	0.45	0.23	0.22

^a BET surface area; ^{b, c} and ^e t-plot method; ^d Volume adsorbed at $P/P_0 = 0.99$; ^f $V_{\text{Meso}} = V_{\text{Total}} - V_{\text{Micro}}$.

2.4. TG-DTA and GC-MS Analysis

The TG-DTA plots of the used HY and HY-H₄EDTA-0.10NH₄OH-0.10TPAOH after 24 h reaction is exhibited in Figure 5A,B. The DTA curves of HY and HY-H₄EDTA-NH₄OH-TPAOH displayed four exothermic peaks in the temperature range of 300 to 1080 K. The first exothermic peak of HY as well as the first and second exothermic peaks of HY-H₄EDTA-NH₄OH-TPAOH were attributed to the desorption of some light components remaining in zeolite pores [11]. The second exothermic peak of HY and the third exothermic peak of HY-H₄EDTA-NH₄OH-TPAOH were attributed to the combustion of soft coke [40,41] that was hemiacetal or methoxyacetyl specie generated during the carbonylation process. The third and fourth exothermic peaks of HY as well as the fourth exothermic peak of HY-H₄EDTA-NH₄OH-TPAOH were attributed to the burning of the heavy coke [42–44]. For the as-used HY, the burnt temperature of soft coke was 682 K and the amount was 5.29%. The heavy coke combustion temperatures were 859 and 1034 K and the amount was 4.43% (3.63% + 0.80%). For HY-H₄EDTA-NH₄OH-TPAOH after 24 h reaction, the soft coke combustion temperature (647 K) and amount (2.42%) as well as the heavy coke burnt temperature (985 K) and amount (0.55%) were lower than those of the parent HY, demonstrating that the coke generation was effectively inhibited in the HY-H₄EDTA-NH₄OH-TPAOH during the carbonylation procedure. The deposition of carbon might be closely relevant to the mesoporous structure and acid strength of the pretreated catalysts [11]. The higher mesoporous surface area and volume, as well as the weaker acid strength, could contribute to the coke reduction. As compared with HY, the HY-H₄EDTA-NH₄OH-TPAOH displayed lower acid strength and greater mesoporous surface area and volume, leading to less generation of carbon deposition.

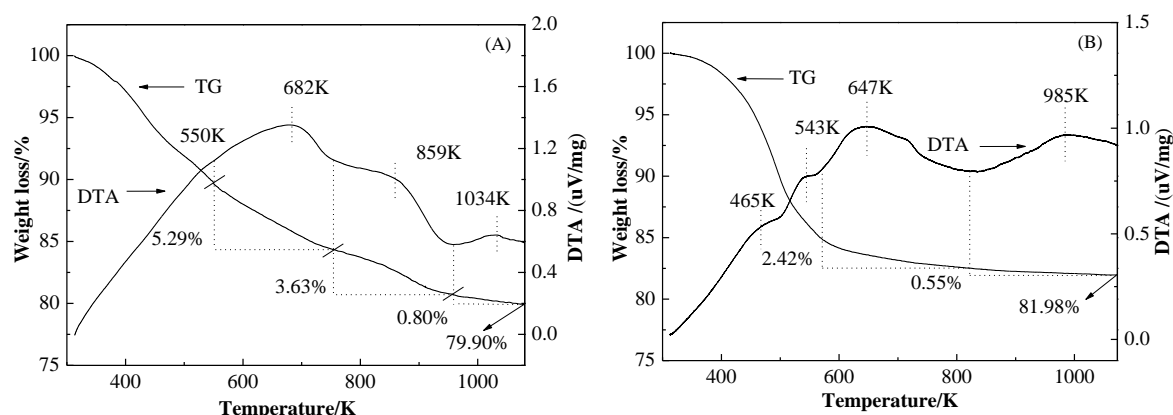


Figure 5. The TG-DTA plots of the used HY (A) and HY-H₄EDTA-NH₄OH-TPAOH (B) zeolites after 24 h reaction.

In order to confirm the coke species of the used HY and HY-H₄EDTA-NH₄OH-TPAOH, about 0.20 g of the catalysts were dissolved with 20% HF solution, and then the coke components were extracted by CH₂Cl₂ solvent. The coke species were identified by GC-MS and shown in Figure 6. For HY after reaction, the coke species mainly included methoxy species, aromatic compounds (anisole, phenol, 2,4-dimethylbenzaldehyde, 2,4-di-tert-butylphenol), nonanal, aliphatic compounds (2,4-dimethylheptane, 5-ethyl-2-methyloctane, C₁₄-C₂₀ alkane), and ester compounds (isopropyl myristate, diisobutyl phthalate, methyl palmitate, isopropyl palmitate, and methyl stearate). For the used HY-H₄EDTA-NH₄OH-TPAOH, the coke species consisted of methoxy species, aromatic compound (anisole, 2,4-dimethylbenzaldehyde, 2,4-di-tert-butylphenol), aliphatic compound (C₂₀ alkane), methyl palmitate, and methyl stearate. It was obvious that the coke species deposited on the HY-H₄EDTA-NH₄OH-TPAOH were extremely less than those of HY, especially the heavy coke species. This result was in good agreement with the former TG-DTA analysis.

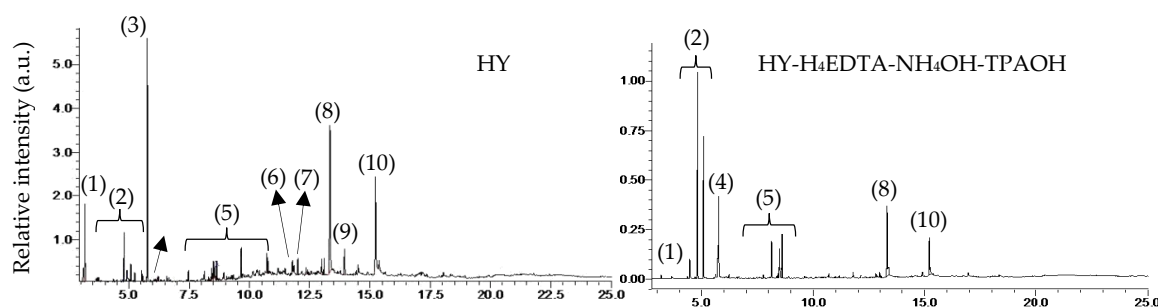


Figure 6. GC-MS analysis of the used HY and HY-H₄EDTA-NH₄OH-TPAOH zeolites after 24 h reaction. The coke species were: (1) methoxy species; (2) aromatic compounds; (3) 2,4-dimethylbenzaldehyde; (4) nonanal; (5) C₁₄-C₂₀ alkane; (6) isopropyl myristate; (7) diisobutyl phthalate; (8) methyl palmitate; (9) isopropyl palmitate; (10) methyl stearate.

2.5. Catalytic Performances of Different Samples for the Carbonylation of DMM

The parent HY and the optimized HY zeolites were used for the DMM carbonylation to MMAc at 100 °C and 5.0 MPa. As displayed in Figure 7A, the DMM conversion was as low as 36.43% for the HY zeolite. After dealumination by H₄EDTA, the DMM conversion of HY-H₄EDTA clearly increased to 51.17%. With the addition of TPABr during H₄EDTA treatment, the DMM conversion of HY-H₄EDTA-TPABr further increased and was as high as 96.29%. After dealumination and further desilication by NaOH, the DMM conversion of HY-H₄EDTA-NaOH was 49.72%. With the introduction of different organic templates (TPAOH, TEOAH, or TMAOH) during NaOH treatment, the DMM conversion of HY-H₄EDTA-NaOH-TPAOH, HY-H₄EDTA-NaOH-TEAOH, and HY-H₄EDTA-NaOH-TMAOH evidently increased to 63.15%, 59.25%, and 55.11%, respectively. As displayed in Figure 7B, when HY-H₄EDTA was treated by NH₄OH for desilication, the DMM conversion of HY-H₄EDTA-NH₄OH was 57.01%. With the addition of different concentrations (0.05–0.20 mol/L) of TPAOH during NH₄OH treatment, the DMM conversion of HY-H₄EDTA-NH₄OH-0.05TPAOH, HY-H₄EDTA-NH₄OH-TPAOH, HY-H₄EDTA-NH₄OH-0.20TPAOH, and HY-H₄EDTA-0.20NH₄OH-TPAOH clearly increased to 88.20%, 95.94%, 96.32%, and 90.09%, respectively. In comparison with the NH₃-TPD analysis in Table 1, the amount of medium-strong acid sites (except for HY-H₄EDTA-NaOH-TEAOH and HY-H₄EDTA-NaOH-TMAOH) were 0.21, 0.32, 0.20, 0.07, 0.25, 0.31, 0.32, 0.26, and 0.23 mmol·g⁻¹. It was clear that the conversion of DMM was consistent with the amount of medium-strong acid sites. This result was in good agreement with our previous report [11], which indicated that higher medium-strong acid sites amount led to higher conversion. Although HY had the largest amount (0.53 mmol·g⁻¹) of medium-strong acid sites, the parent HY exhibited the lowest DMM conversion. This could be attributed to the lower mass-transfer efficiency because of the microporous structure.

As shown in Figure 7A, the parent HY exhibited only 11.06% selectivity of MMAc. When HY was treated by H₄EDTA for dealumination, the MMAc selectivity of HY-H₄EDTA sharply increased to 85.55%. After dealumination by H₄EDTA and TPABr, the MMAc selectivity of HY-H₄EDTA-TPABr further improved and reached 91.92%. When the HY-H₄EDTA was treated by NaOH for desilication, the MMAc selectivity of HY-H₄EDTA-NaOH was as low as 10.65%, much lower than that of HY because a high concentration of NaOH resulted in the fractional collapse of the zeolitic structure [28]. With the addition of TPAOH, TEOAH, or TMAOH during NaOH treatment, the MMAc selectivity of HY-H₄EDTA-NaOH-TPAOH, HY-H₄EDTA-NaOH-TEAOH, and HY-H₄EDTA-NaOH-TMAOH obviously increased to 87.37%, 82.72%, and 80.52%, respectively. As exhibited in Figure 7B, after dealumination and further desilication by NH₄OH, the MMAc selectivity of HY-H₄EDTA-NH₄OH was 81.44%. When HY-H₄EDTA was treated by NH₄OH and different concentrations of TPAOH for desilication, the MMAc selectivity of HY-H₄EDTA-NH₄OH-0.05TPAOH, HY-H₄EDTA-NH₄OH-TPAOH, HY-H₄EDTA-NH₄OH-0.20TPAOH, and HY-H₄EDTA-0.20NH₄OH-TPAOH evidently improved to 86.25%, 92.04%, 92.35%, and 85.17%, respectively. We believe that the efficiency of mass transfer and the

diffusion of MMAc were highly limited in microporous HY zeolite due to its high molecular weight. Accordingly, the lower mass transfer efficiency could cause residue of the heavy products on the acid sites, leading to the generation of the carbon deposition, which easily resulted in the deactivation of the catalyst. Therefore, the optimized HY zeolites with greater mesopore volume and surface area obviously improved the efficiency of mass transfer, resulting in the improvement of MMAc selectivity.

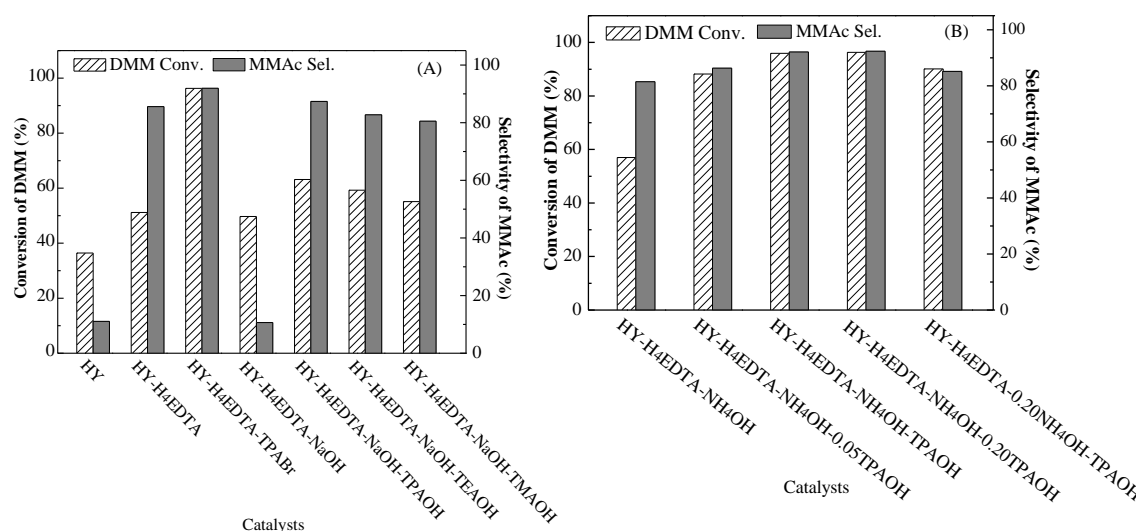


Figure 7. The effect of different catalysts (A) and (B) on the carbonylation of dimethoxymethane (DMM) to methyl methoxyacetate (MMAc). Reaction conditions: catalyst weight, 1.0 g; reaction temperature, 100 °C; reaction pressure, 5.0 MPa; total CO flow rate, 100 mL/min; time on stream, 2 h.

2.6. Catalytic Stability of HY, HY-H₄EDTA-NH₄OH, and HY-H₄EDTA-NH₄OH-TPAOH

The stability of HY, HY-H₄EDTA-0.10NH₄OH, and HY-H₄EDTA-NH₄OH-TPAOH was conducted under the same conditions. The DMM conversion and the MMAc selectivity with 24 h reaction is exhibited in Figure 8. At the initial 10 h, the conversion of HY rapidly decreased from 37.15% to 17.96%, and the MMAc selectivity remained nearly unchanged at about 11.06%. After 10 h reaction, the parent HY gradually lost its performance from 17.96% to 9.19% until 24 h when the selectivity of MMAc slowly decreased from 11.06% to 10.71%. For HY-H₄EDTA-NH₄OH, the variation trend of DMM conversion was almost consistent with that of HY, and rapidly declined from 57.16% to 43.04% at the initial 10 h and further dropped to 39.60% after 24 h reaction. The selectivity of HY-H₄EDTA-NH₄OH remained at a constant value of about 81.44% during 24 h reaction, much higher than that of HY, since the efficiency of mass transfer clearly improved due to the increased mesoporous surface area and volume. For HY-H₄EDTA-NH₄OH-TPAOH, it was obvious that the DMM conversion (95.94%) and the MMAc selectivity (92.04%) stayed almost unchanged even through 24 h reaction, showing that the behavior of the optimized HY-H₄EDTA-NH₄OH-TPAOH zeolite was extremely stable. We considered that the superior performance and stability of HY-H₄EDTA-NH₄OH-TPAOH were attributed to the increased medium-strong acid sites amount as well as the improved efficiency of mass transfer in mesoporous structure. The reason for the deactivation of the catalysts was attributed to the carbon deposition because all the components in this study system were neutral and would not result in the removal of aluminum and silicon from the framework. The TG-DTA and GC-MS analysis also revealed that HY-H₄EDTA-NH₄OH-TPAOH was counteractive to the generation of coke. Hence, the optimized HY-H₄EDTA-NH₄OH-TPAOH zeolite displayed higher mass transfer efficiency, leading to outstanding stability during 24 h reaction.

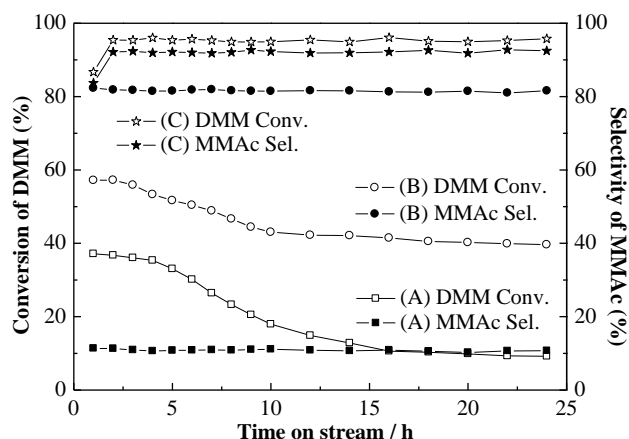


Figure 8. The catalytic stability of HY (A), HY-H₄EDTA-NH₄OH (B), and HY-H₄EDTA-NH₄OH-TPAOH (C) for 24 h reaction. Reaction conditions: catalyst weight, 1.0 g; reaction temperature, 100 °C; reaction pressure, 5.0 MPa; total CO flow rate, 100 mL/min; time on stream, 24 h.

3. Materials and Methods

3.1. Materials

The parent HY zeolite (Si/Al = 2.7) was purchased from Nankai University Catalyst Co. Sodium hydroxide (NaOH, 98%), Ethylenediaminetetraacetic acid (H₄EDTA, 99%), ammonium nitrate (NH₄NO₃, 99%), and ammonia aqueous solution (NH₄OH) were obtained from Sinopharm Chemical Reagent Co., Ltd. Dimethoxymethane (DMM, 98%) was acquired from Sigma–Aldrich. Four organic templates, including tetrapropyl ammonium bromide (TPABr, 99%), tetrapropyl ammonium hydroxide (TPAOH, 99%), tetraethyl ammonium hydroxide (TEAOH, 99%), and tetramethyl ammonium hydroxide (TMAOH, 99%) were provided by Aladdin Co. All the reagents were directly used without further purification.

3.2. Catalyst Preparation

Dealumination: 13.40 g parent HY zeolite was first put into 200 mL 0.11 mol/L H₄EDTA or the mixed solution of 0.11 mol/L H₄EDTA and 0.10 mol/L TPABr, followed by stirring at 65 °C for 6 h. The suspension was filtered and washed until the pH value was 7.0. The desired sample was dried at 120 °C for 8 h and then calcined at 550 °C for 4 h to acquire the precursor, noted as “HY-H₄EDTA” and “HY-H₄EDTA-TPABr”.

Desilication: 1.70 g HY-H₄EDTA was poured into a 50 mL mixed solution of 0.10 or 0.20 mol/L alkali (NaOH or NH₄OH) and 0.05–0.20 mol/L PDAs (TPABr, TPAOH, TEAOH, and TMAOH), followed by stirring at 65 °C for 0.5 h. The suspension was also filtered and washed until the pH value was 7.0. The obtained solid was dried at 120 °C and afterwards calcined in a muffle furnace at 550 °C for 4 h to gain the precursor. The NaOH and PDA treatments were noted as “HY-H₄EDTA-NaOH-PDA”, while the NH₄OH and PDA treatments were labeled as “HY-H₄EDTA-NH₄OH-PDA”.

After treatments of dealumination and desilication, 10 g of the precursor was exchanged with 1.0 mol/L NH₄NO₃ solution at 65 °C in order to convert it into the NH₄⁺ form. The suspension was filtered and washed several times. The obtained precursor was dried at 120 °C, subsequently calcined at 550 °C for 6 h in a muffle furnace to receive the catalyst.

3.3. Catalyst Characterization

Powder X-ray diffraction (XRD) patterns were obtained with a Bruker D8 advance diffractometer using Cu K α (λ = 0.15406 nm) radiation. Data was recorded in the 2 θ range from 5 to 40° with a step size of 0.05° at 40 kV and 40 mA. The relative crystallinity of the as-treated HY zeolites was

calculated by comparing the relative intensity divided by the reference at 2θ of 23.58° , assuming that the crystallinity of reference HY was 100% [12].

N_2 isotherms were measured in a Quantachrome (Autosorb iQ Statio) instrument at 77 K. The samples were first treated at 300°C under vacuum for 3 h. The surface area was calculated by using a Brunauer–Emmett–Teller (BET) method. Barrett–Joyner–Halenda (BJH) and Horváth–Kawazoe (HK) methods were applied to determine the pore size distribution in the mesopore and micropore region, respectively.

The NH_3 -TPD experiments were carried out on a Builder PCA-1200. 200 mg sample was pretreated at 300°C in a flow of 30 mL/min He for 1 h. After the pretreatment, the sample was cooled to 80°C and exposed to NH_3 for 10 min. Then, the physically adsorbed NH_3 was removed by He at the same temperature until the baseline was stable. Thereafter, NH_3 -TPD was conducted in a constant flow of He (30 mL/min) from 80 to 700°C at a heating rate of $10^\circ\text{C}/\text{min}$. The amount of desorbed NH_3 was detected by a thermal conductivity detector.

TG-DTA analysis proceeded in the thermal analysis equipment (STA 449C Jupiter, NETZSCH). 2 mg precursor was performed in a flow of 80 mL/min air with the temperature increasing from 40 to 800°C at a heating rate of $10^\circ\text{C}/\text{min}$.

The coke species were analyzed by GC-MS. First, about 0.2 g of the catalyst was dried at 200°C for 1 h, then the sample was dissolved with 2 mL of 20% hydrofluoric acid (HF) solution according to the literature [45]. The coke species were extracted with dichloromethane (CH_2Cl_2) and were subsequently analyzed on a GCMS-TQ8040 instrument. The coke species were obtained by comparing chromatographic peaks with the NIST14 database.

3.4. Catalyst Test

The carbonylation reaction was conducted in a continuous fixed-bed reactor with an inner diameter of 8.5 mm by employing 1.0 g of the catalyst at 100°C and 5.0 MPa CO pressure. 20 mL/min CO bubbled through a stainless-steel saturator filled with DMM kept at 25°C , and 80 mL/min pure CO were mixed together and introduced into the reactor. All the reaction products were analyzed online by a gas chromatograph (GC-2014C) equipped with a HP-FFAP capillary column connected to a flame ionization detector. The conversion of DMM and the MMAc selectivity were calculated on the basis of weight, as follows [11,46]: $DMM\text{ Conv.} = (DMM_{in} - DMM_{left})/DMM_{in}$; MMAc selectivity was calculated on the basis of weight, $MMAc\text{ Sel.} = MMAc_{formation}/\text{the mass of all products}$.

4. Conclusions

A series of organic templates (TPABr, TPAOH, TEAOH, and TMAOH) were added during the dealumination or desilication process to optimize the pore structures of hierarchical HY zeolites. The XRD analysis revealed that the optimized HY zeolites displayed much higher relative crystallinity than that of hierarchical HY zeolites produced in the absence of templates. According to the N_2 adsorption-desorption analysis, both the large mesopore size and amount of the optimized HY zeolites remained nearly unchanged, while the micropore amount clearly increased, showing that the introduced templates largely protected microporous structure. The NH_3 -TPD analysis showed that the introduction of templates during dealumination or desilication process could increase the medium-strong acid sites amount of as-treated HY zeolites. The conversion of DMM was strictly in accordance with the amount of medium-strong acid sites, and higher acid amount resulted in higher DMM conversion. The optimized HY zeolites displayed superior conversion of DMM and selectivity of MMAc since the larger mesoporous surface area and volume contributed to increasing the efficiency of mass transfer, resulting in significantly less carbon deposition. It was proved by TG-DTA and GC-MS analyses that the generation of coke was effectively inhibited. HY- $H_4EDTA-NH_4OH$ -TPAOH exhibited outstanding performance (95.94% DMM conversion and 92.04% MMAc selectivity) and stability at 100°C and 5.0 MPa during 24 h reaction procedure. This optimized HY zeolite, which was highly active and stable, exhibited tremendous potential for the industrial production of MMAc.

Author Contributions: Conceptualization and methodology, F.C., D.Z., L.S., and G.X.; investigation, F.C., D.Z., and Y.W.; writing—original draft preparation, F.C. and D.Z.; writing—review and editing, L.S. and G.X.

Funding: This research was funded by the Liaoning Provincial University Innovation Talent Project (LR 2016015).

Acknowledgments: The authors are grateful for the financial support from the Liaoning Provincial University Innovation Talent Project (LR 2016015).

Conflicts of Interest: The authors declare no conflict of interest.

References

1. Ivanova, I.I.; Kuznetsov, A.S.; Yuschenko, V.V.; Knyazeva, E.E. Design of composite micro/mesoporous molecular sieve catalysts. *Pure Appl. Chem.* **2004**, *76*, 1647–1657. [[CrossRef](#)]
2. Xing, C.; Sun, J.; Yang, G.H.; Shen, W.Z.; Tan, L.; Zhu, P.F.; Wei, Q.H.; Li, J.; Kyodo, M.; Yang, R.Q.; et al. Tunable isoparaffin and olefin synthesis in Fischer–Tropsch synthesis achieved by composite catalyst. *Fuel Process. Technol.* **2015**, *136*, 68–72. [[CrossRef](#)]
3. Gueudré, L.; Milina, M.; Mitchell, S.; Pérez-Ramírez, J. Superior mass transfer properties of technical zeolite bodies with hierarchical porosity. *Adv. Funct. Mater.* **2014**, *24*, 209–219. [[CrossRef](#)]
4. Lei, Q.; Zhao, T.B.; Li, F.Y.; Zhang, L.L.; Wang, Y. Catalytic cracking of large molecules over hierarchical zeolites. *Chem. Commun.* **2006**, *16*, 1769–1771. [[CrossRef](#)] [[PubMed](#)]
5. Sun, Y.Y.; Prins, R. Friedel–Crafts alkylations over hierarchical zeolite catalysts. *Appl. Catal. A Gen.* **2008**, *336*, 11–16. [[CrossRef](#)]
6. Li, Y.X.; Huang, Y.H.; Guo, J.H.; Zhang, M.Y.; Wang, D.Z.; Wei, F.; Wang, Y. Hierarchical SAPO-34/18 zeolite with low acid site density for converting methanol to olefins. *Catal. Today* **2014**, *233*, 2–7. [[CrossRef](#)]
7. Kim, S.H.; Chun, D.B.; Yoon, S.D.; Byun, H.S. Phase Behavior for the CO₂ + Methyl Methoxyacetate and CO₂ + Methyl trans-3-Methoxyacrylate Systems at Pressures from (5 to 20) MPa and Various Temperatures. *J. Chem. Eng. Data* **2016**, *61*, 1101–1108. [[CrossRef](#)]
8. Balkenhohl, F.; Ditrach, K.; Hauer, B.; Ladner, W. Optisch aktive amine durch lipase-katalysierte methoxyacetylierung. *J. Prakt. Chem.* **1997**, *339*, 381–384. [[CrossRef](#)]
9. Celik, F.E.; Kim, T.J.; Bell, A.T. Effect of zeolite framework type and Si/Al ratio on dimethoxymethane carbonylation. *J. Catal.* **2010**, *270*, 185–195. [[CrossRef](#)]
10. Yue, H.R.; Zhao, Y.J.; Ma, X.B.; Gong, J.L. Ethylene glycol: Properties, synthesis, and applications. *Chem. Soc. Rev.* **2012**, *41*, 4218–4244. [[CrossRef](#)]
11. Zhang, D.X.; Shi, L.; Wang, Y.; Chen, F.; Yao, J.; Li, X.Y.; Ni, Y.M.; Zhu, W.L.; Liu, Z.M. Effect of mass-transfer control on HY zeolites for dimethoxymethane carbonylation to methyl methoxyacetate. *Catal. Today* **2018**, *316*, 114–121. [[CrossRef](#)]
12. Verboekend, D.; Vilé, G.; Pérez-Ramírez, J. Hierarchical Y and USY zeolites designed by post-synthetic strategies. *Adv. Funct. Mater.* **2012**, *22*, 916–928. [[CrossRef](#)]
13. Groen, J.C.; Abelló, S.; Villaescusa, L.A.; Pérez-Ramírez, J. Mesoporous beta zeolite obtained by desilication. *Microporous Mesoporous Mater.* **2008**, *114*, 93–102. [[CrossRef](#)]
14. Čížmek, A.; Subotić, B.; Aiello, R.; Crea, F.; Nastro, A.; Tuoto, C. Dissolution of high-silica zeolites in alkaline solutions I. Dissolution of silicalite-1 and ZSM-5 with different aluminum content. *Microporous Mater.* **1995**, *4*, 159–168.
15. Verboekend, D.; Pérez-Ramírez, J. Desilication mechanism revisited: Highly mesoporous all-silica zeolites enabled through pore-directing agents. *Chem. Eur. J.* **2011**, *17*, 1137–1147. [[CrossRef](#)] [[PubMed](#)]
16. Verboekend, D.; Milina, M.; Mitchell, S.; Pérez-Ramírez, J. Hierarchical zeolites by desilication: Occurrence and catalytic impact of recrystallization and restructuring. *Cryst. Growth Des.* **2013**, *13*, 5025–5035. [[CrossRef](#)]
17. Verboekend, D.; Nuttens, N.; Locus, R.; Van Aelst, J.; Verolme, P.; Groen, J.C.; Pérez-Ramírez, J.; Sels, B.F. Synthesis, characterisation, and catalytic evaluation of hierarchical faujasite zeolites: Milestones, challenges, and future directions. *Chem. Soc. Rev.* **2016**, *45*, 3331–3352. [[CrossRef](#)]
18. Liu, H.; Xie, S.J.; Xin, W.J.; Liu, S.L.; Xu, L.Y. Hierarchical ZSM-11 zeolite prepared by alkaline treatment with mixed solution of NaOH and CTAB: Characterization and application for alkylation of benzene with dimethyl Ether. *Catal. Sci. Technol.* **2016**, *6*, 1328–1342. [[CrossRef](#)]
19. Verboekend, D.; Vilé, G.; Pérez-Ramírez, J. Mesopore formation in USY and beta zeolites by base leaching: Selection criteria and optimization of pore-directing agents. *Cryst. Growth Des.* **2012**, *12*, 3123–3132. [[CrossRef](#)]

20. Van laak, A.N.C.; Zhang, L.; Parvulescu, A.N.; Bruijninx, P.C.A.; Weckhuysen, B.M.; de Jong, K.P.; de Jongh, P.E. Alkaline treatment of template containing zeolites: Introducing mesoporosity while preserving acidity. *Catal. Today* **2011**, *168*, 48–56. [[CrossRef](#)]
21. De Jong, K.P.; Zečević, J.; Friedrich, H.; de Jongh, P.E.; Bulut, M.; van Donk, S.; Kenmogne, R.; Finiels, A.; Hulea, V.; Fajula, F. Zeolite Y crystals with trimodal porosity as ideal hydrocracking catalysts. *Angew. Chem. Int. Ed.* **2010**, *49*, 10074–10078. [[CrossRef](#)] [[PubMed](#)]
22. García-Martínez, J. Introduction of Mesoporosity into Inorganic Materials in The Presence of a Non-ionic Surfactant. US 20130183229A1, 18 July 2013.
23. Ghosh, M.; Lohrasbi, M.; Chuang, S.S.C.; Jana, S.C. Mesoporous titanium dioxide nanofibers with a significantly enhanced photocatalytic activity. *ChemCatChem* **2016**, *8*, 2525–2535. [[CrossRef](#)]
24. Liu, Z.H.; Hua, Y.J.; Wang, J.J.; Dong, X.L.; Tian, Q.W.; Han, Y. Recent progress in the direct synthesis of hierarchical zeolites: Synthetic strategies and characterization methods. *Mater. Chem. Front.* **2017**, *1*, 2195–2212. [[CrossRef](#)]
25. Bai, R.S.; Song, Y.; Li, Y.; Yu, J.H. Creating Hierarchical Pores in Zeolite Catalysts. *Trends Chem.* **2019**, *1*, 601–611. [[CrossRef](#)]
26. Sing, K.S.W.; Everett, D.H.; Haul, R.A.W.; Moscou, L.; Pierotti, R.A.; Rouquerol, J.; Siemieniewska, T. Reporting physisorption data for gas/solid systems—with special reference to the determination of surface area and porosity. *Pure Appl. Chem.* **1985**, *57*, 603–619. [[CrossRef](#)]
27. Perez-Ramirez, J.; Abello, S.; Villaescusa, L.A.; Bonilla, A. Toward Functional Clathrasils: Size-and Composition-Controlled Octadecasil Nanocrystals by Desilication. *Angew. Chem. Int. Ed.* **2008**, *47*, 7913–7917. [[CrossRef](#)] [[PubMed](#)]
28. Suzuki, T.; Okuhara, T. Change in pore structure of MFI zeolite by treatment with NaOH aqueous solution. *Microporous Mesoporous Mater.* **2001**, *43*, 83–89. [[CrossRef](#)]
29. Li, X.; Shantz, D.F. PFG NMR Investigations of Tetraalkylammonium—Silica Mixtures. *J. Phys. Chem. C* **2010**, *114*, 8449–8458. [[CrossRef](#)]
30. Zheng, J.J.; Yi, Y.M.; Wang, W.L.; Guo, K.; Ma, J.H.; Li, R.F. Synthesis of bi-phases composite zeolites MFZ and its hierarchical effects in isopropylbenzene catalytic cracking. *Microporous Mesoporous Mater.* **2013**, *171*, 44–52. [[CrossRef](#)]
31. Yang, G.H.; Tsubaki, N.; Shamoto, J.; Yoneyama, Y.; Zhang, Y. Confinement Effect and Synergistic Function of H-ZSM-5/Cu-ZnO-Al₂O₃ Capsule Catalyst for One-Step Controlled Synthesis. *J. Am. Chem. Soc.* **2010**, *132*, 8129–8136. [[CrossRef](#)]
32. Jin, D.F.; Zhu, B.; Hou, Z.Y.; Fei, J.H.; Lou, H.; Zheng, X.M. Dimethyl ether synthesis via methanol and syngas over rare earth metals modified zeolite Y and dual Cu–Mn–Zn catalysts. *Fuel* **2007**, *86*, 2707–2713. [[CrossRef](#)]
33. Yaripour, F.; Baghaei, F.; Schmidt, I.; Perregaard, J. Catalytic dehydration of methanol to dimethyl ether (DME) over solid-acid catalysts. *Catal. Commun.* **2005**, *6*, 147–152. [[CrossRef](#)]
34. Arena, F.; Dario, R.; Parmaliana, A. A characterization study of the surface acidity of solid catalysts by temperature programmed methods. *Appl. Catal. A Gen.* **1998**, *170*, 127–137. [[CrossRef](#)]
35. Taufiqurrahmi, N.; Mohamed, A.R.; Bhatia, S. Nanocrystalline zeolite beta and zeolite Y as catalysts in used palm oil cracking for the production of biofuel. *J. Nanoparticle Res.* **2011**, *13*, 3177–3189. [[CrossRef](#)]
36. Wang, L.; Wang, Y.; Wang, A.; Li, X.; Zhou, F.; Hu, Y. Highly acidic mesoporous aluminosilicates assembled from zeolitic subunits generated by controllable desilication of ZSM-5 in Na₂SiO₃ solution. *Microporous Mesoporous Mater.* **2013**, *180*, 242–249. [[CrossRef](#)]
37. Cranston, R.W.; Inkley, F.A. The determination of pore structures from nitrogen adsorption isotherms. *Adv. Catal.* **1957**, *9*, 143–154.
38. Verboekend, D.; Pérez-Ramírez, J. Design of hierarchical zeolite catalysts by desilication. *Catal. Sci. Technol.* **2011**, *1*, 879–890. [[CrossRef](#)]
39. Pérez-Ramírez, J.; Verboekend, D.; Bonilla, A.; Abelló, S. Zeolite catalysts with tunable hierarchy factor by pore-growth moderators. *Adv. Funct. Mater.* **2009**, *19*, 3972–3979. [[CrossRef](#)]
40. Shi, L.; Yao, J.; Zhu, W.L.; Liu, Z.M. Efficient sulfonic acid resin catalysts for carbonylation of dimethoxymethane to value-added methyl methoxyacetate. *J. CIESC* **2017**, *68*, 3739–3746.
41. Shapovalov, V.; Bell, A.T. Theoretical study of zeolite-catalyzed dimethoxymethane carbonylation to methyl methoxyacetate. *J. Phys. Chem. C* **2010**, *114*, 17753–17760. [[CrossRef](#)]

42. Cambor, M.A.; Corma, A.; Valencia, S. Characterization of nanocrystalline zeolite Beta. *Microporous Mesoporous Mater.* **1998**, *25*, 59–74. [[CrossRef](#)]
43. Guisnet, M.; Magnoux, P. Organic chemistry of coke formation. *Appl. Catal. A Gen.* **2001**, *212*, 83–96. [[CrossRef](#)]
44. Palumbo, L.; Bonino, F.; Beato, P.; Bjørgen, M.; Zecchina, A.; Bordiga, S. Conversion of methanol to hydrocarbons: Spectroscopic characterization of carbonaceous species formed over H-ZSM-5. *J. Phys. Chem. C* **2008**, *112*, 9710–9716. [[CrossRef](#)]
45. Guisnet, M.; Costa, L.; Ribeiro, F.R. Prevention of zeolite deactivation by coking. *J. Mol. Catal. A Chem.* **2009**, *305*, 69–83. [[CrossRef](#)]
46. Chen, F.; Shi, L.; Yao, J.; Wang, Y.; Zhang, D.X.; Zhu, W.L.; Liu, Z.M. A highly efficient sulfonic acid resin for liquid-phase carbonylation of dimethoxymethane. *Catal. Sci. Technol.* **2018**, *8*, 580–590. [[CrossRef](#)]



© 2019 by the authors. Licensee MDPI, Basel, Switzerland. This article is an open access article distributed under the terms and conditions of the Creative Commons Attribution (CC BY) license (<http://creativecommons.org/licenses/by/4.0/>).